Two-photon excitation spectra of divalent europium in cubic perovskite $KMgF_3$

R. Francini, U. M. Grassano, and M. Tomini
Dipartimento di Fisica and Istituto Nazionale di Fisica della Materia, Università di Roma ''Tor Vergata,'' Via della Ricerca Scientifica 1, 00133 Roma, Italy

S. Boiko and G. G. Tarasov
Institute of Semiconductor Physics of the National Academy of Science of Ukraine, Prospect Nauki 45, 252 Kiev, Ukraine

A. Scacco
Dipartimento di Fisica and Istituto Nazionale di Fisica della Materia, Università di Roma ''La Sapienza,'' Piazzale Aldo Moro 2, 00185 Roma, Italy

(Received 25 January 1996; revised manuscript received 12 June 1996)

Intraconfigurational $4f^7$ transitions of Eu^{2+} in $KMgF_3$ have been investigated by means of two-photon excitation spectroscopy. A well-resolved Stark structure of the $^8S_{7/2} \rightarrow {}^6P_{7/2,5/2}$ transitions is demonstrated and interpreted. Additional lines appearing in the excitation spectra are discussed in terms of noncubic perturbations at the substitutional impurity site. $4f^7$ excited states of Eu^{2+} belonging to the ^6D multiplet, inaccessible to single-photon spectroscopy, have been identified in $KMgF_3$. [S0163-1829(97)00111-2]

I. INTRODUCTION

Rare-earth ions in insulating crystals have been extensively studied with the technique of two-photon excitation (TPE) spectroscopy. The electronic properties of these ionic impurities are indeed appealing to nonlinear spectroscopy, due to several features: the energy range of the exciting source needs to span the visible and near infrared, where dye lasers perform at their best; the two-photon-allowed transitions take place between states weakly coupled to the crystal lattice, yielding unusually narrow ultraviolet excitation lines [in some cases the linewidth is less than 10 GHz (Ref. 1)] with well-resolved Stark components. Among the rare earths, characterized by the progressive filling of the $4f$ shell of their electronic configuration, divalent europium presents the most complicated case of a half-filled shell. In the scheme of pure LS coupling, all first-order crystal-field separations of the f configuration multiplets should vanish. The observed splittings can be ascribed to intermediate coupling which includes, besides the electrostatic interactions, magnetic couplings like spin-orbit, spin-spin and spin-other-orbit.[2–5] When the Eu^{2+} ions are immersed into a crystal lattice, additional interactions need to be considered which strongly affect the energy spectrum of the rare-earth ion, the probability of intrashell transitions, and the width of the electronic levels.

Comprehensive experimental data are available about the energy spectrum of Eu^{2+} in different crystals. The $^6P_{7/2,5/2}$ levels were observed in the one-photon spectrum of Eu^{2+} in $KMgF_3$,[6–8] alkaline-earth sulfates,[9] and ternary alkaline-earth aluminum fluorides.[10] In these crystals $^6P_{7/2,5/2}$ states occur below the onset of the $4f^6 5d$ absorption band edge, and can be seen in absorption and emission as narrow lines corresponding to the transitions $^8S_{7/2} \rightarrow {}^6P_{7/2,5/2}$. Emission and one-photon excitation to the ^6I levels of Eu^{2+} in $KMgF_3$ have also been observed.[8] It is evident that the lowest excited $4f^6 5d$ level is in this case situated above the $^6I_{7/2}$ level, which is the lowest component of the ^6I_J manifold.

On the other hand, in cubic alkaline-earth fluorides[11] and alkali halides,[12] the excited $4f^6 5d$ configuration is in a position where it completely overlaps even the lowest $4f^7$ excited states, which lie in the near ultraviolet. Only the intense broad bands arising from the electric-dipole allowed $4f^7 \rightarrow 4^6 5d$ interconfigurational transitions can be expected in the one-photon absorption spectrum. These transitions, however, are forbidden in second order due to the parity selection rule, allowing the sharp intraconfigurational $4f^7 \rightarrow 4f^7$ transitions to be observed in two-photon absorption processes. A comprehensive analysis of numerous direct two-photon transitions of Eu^{2+} in CaF_2 and SrF_2 was performed by Downer and co-workers.[11,13] In order to interpret the relative intensities and the polarization anisotropies of the intrashell transitions, it is necessary to determine the maximum number of energy levels experimentally. In this way, one has the possibility of extracting from the data the parameters characterizing the crystal field at the ion and the symmetry of the sites, as well as the wave functions of different states, which are needed to calculate the intensity of optical transitions.

In the case of Eu^{2+} ions in $KMgF_3$, the spectra of the excited $4f^7$ states are partially known. Even if two extensive sets of data exist for this system,[7,8] they are not completely consistent with respect to one another: the wave numbers of the observed lines, their intensities, and the number and symmetry of the substitutional sites are interpreted in a somewhat different way.

In this work we present data concerning the behavior of Eu^{2+} ions in perovskite $KMgF_3$. TPE spectra of high-quality and previously unattained resolution show rich Stark structures for each of the ^6P and ^6D J multiplets, originated from the crystal-field splitting for different site symmetries of Eu^{2+} in the unit cell of the cubic crystal. The temperature and polarization dependence of ^6D multiplets found in per-

ovskite show a significant mixing of the higher excited electronic states induced by the host crystal. A preliminary assignment of different Stark components is performed based on a simplified calculation of crystal-field influence. In addition to dominating features ascribed to cubic Eu^{2+} centers in $KMgF_3$, we have also obtained from the excitation spectra clear evidence of the existence of trigonal centers. The $B_0^{(4)}$ and $B_0^{(6)}$ coefficients of cubic crystal field are fitted to the experimental $^6P_{7/2}$ and $^6P_{5/2}$ splittings in the twelvefold fluorine environment of Eu^{2+}.

II. EXPERIMENT

$KMgF_3$:Eu^{2+} single crystals were grown from the melt with the Kyropoulos method in an inert atmosphere, starting from stoichiometric mixtures of KF and MgF_2 dehydrated powders added to various amounts of $EuCl_3$, and subsequently temperature annealed to eliminate any trace of Eu^{3+}. The single-crystal samples were cut and polished from the crystal boules (a typical diameter of 2.5 cm and a length of 3 cm) along (100) planes, to a final size of approximately $1\times0.5\times0.5$ cm^3. $KMgF_3$ crystals belong to the space group O_h, with the cubic unit cell where the F^- ions are located at the center of each face, Mg^{2+} ions are found at the center of each cube, and the K^+ ions occupy the vertices of the cube. Eu^{2+} ions enter substitutionally into the crystal, replacing a singly charged cation K^+ in the perovskite lattice.[7,8] Such a replacement, which is favored by the similarity of the ionic radii of K^+ and Eu^{2+} ions, needs an additional point defect in order to compensate for the excess of charge. No evidence of the existence of Eu^{3+} in the samples we used in the present work has been deduced from the optical properties, whereas several additional lines appear in the TPE spectra with increasing Eu concentration in the melt.

The two-photon transitions were detected by monitoring the luminescence at 359 nm, which follows the excitation process. The exciting source was a dye-laser pumped by an excimer laser operating at 308-nm wavelength (XeCl gas mixture). The repetition rate was 20 Hz, with pulses of 8–10-ns duration (depending on employed dye and wavelength) and peak powers ranging from 200 to 350 kW. The dye-laser oscillator, without intracavity etalon, produces a bandwidth of 0.18 cm^{-1} at 710 nm, which increases to 0.2 cm^{-1} at 580 nm. The laser bandwidth sets the lower limit to our measurements of the low-temperature TPE linewidths. The laser beam was weakly focused inside the sample, mounted in a variable-temperature (15–300 K) cryostat. The luminescence following the two-photon excitation was collected at 90° with respect to the incident laser beam, and, after proper filtering with Schott-glass color filters, detected with a single-photon-counting setup. The signal was averaged over a number of laser shots varying from 50 to 100 for each wavelength, and then normalized to the square of the laser-pulse intensity. The laser-pulse intensity was monitored with a fast photodiode, and read shot by shot with a gated digitizing charge integrator. All TPE spectra presented here were measured with the laser beam linearly polarized parallel to the [010] crystal axis and propagating along the [001] direction. A Soleil-Babinet compensator or a combination of a Soleil-Babinet compensator and a Glan polarizer allowed for the choice of the laser-beam polarization state and polarization direction, respectively, when the measurements of the two-photon excited luminescence as a function of the polarization of the exciting beam were carried out.

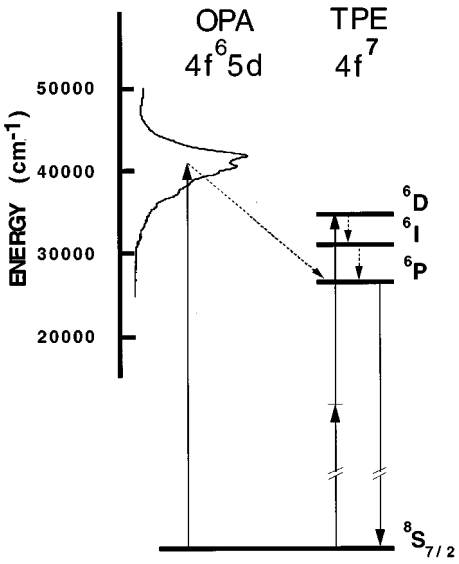

FIG. 1. Schematic diagram of the lower-energy levels of Eu^{2+} in $KMgF_3$ showing two-photon excitation (TPE), relaxation, and recombination luminescence. The one-photon absorption (OPA) spectrum is drawn for comparision on the left-hand side.

III. RESULTS AND DISCUSSION

A. Two-photon excitation of $^8S_{7/2}\rightarrow{}^6P_J$ transitions

Figure 1 provides a sketch of the relevant optical transitions discussed in the present work, together with the one-photon absorption spectrum. Two-photon transitions were induced from the $^8S_{7/2}$ ground state of the Eu^{2+} to the ^6P_J multiplet belonging to the $4f^7$ electronic configuration. In the same ion, one-photon allowed transitions take place from the ground state to the $4f^6 5d$ excited states, with broad absorption bands characterized by several structures, due to crystal-field splitting and strong coupling with local vibrations. In the $KMgF_3$ perovskite the $4f^6 5d$ state lies about 3000 cm^{-1} higher in energy than the $4f^7(^6P_J)$ multiplet, and the lowest $4f^6 5d$ levels are just about 100 cm^{-1} above the $4f^7(^6I)$ multiplets.[8] Due to rapid, nonradiative decay to the lowest excited $4f^7$ multiplet from all higher states, at low temperature fluorescence is almost entirely emitted from the $^6P_{7/2}$ state, the lowest component of the ^6P_J multiplet. When the temperature is increased, fluorescence has also been observed from the $^6P_{5/2}$ component.[7] These emissions are characterized by very narrow linewidths (zero-phonon lines) and milliseconds decay-time constants.

Our TPE measurements of Eu^{2+} in $KMgF_3$ span the range of the ^6P_J and ^6D_J multiplets. Due to the high resolution, each one of the spectra shown in the following figures covers only a narrow energy region around each J multiplet. The TPE spectrum of the $^6P_{7/2}$ levels showing the fully resolved Stark structure is reported in Fig. 2. The lines marked with Γ_6, Γ_7, and Γ_8 are those identified as belonging to the ion in a cubic environment, where a $J=\frac{7}{2}$ state is split into

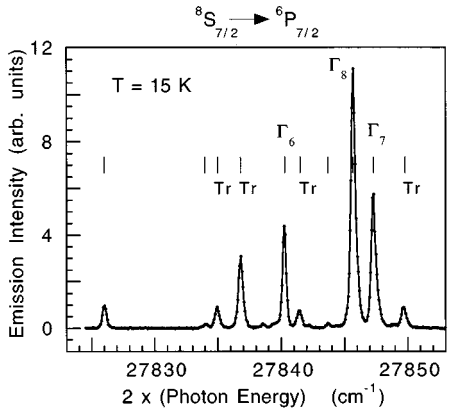

FIG. 2. Two-photon excitation spectrum of $KMgF_3$: Eu^{2+} in the $^8S_{7/2} \rightarrow {}^6P_{7/2}$ spectral range. The laser beam is linearly polarized parallel to the [010] crystal axis.

three levels. The intensity ratios of the three lines are in good agreement with those expected from the degeneracy of the final state, and are insensible to a change in Eu concentration. Other lines appear in the spectra: their relative intensities depend on the Eu content, and their energy positions are exactly reproducible. This suggests the existence of different possible sites for the impurity and although the majority of the divalent europium ions enters substitutionally in the crystal at a cubic site, other lattice sites of lower symmetry are available to europium.

Figure 3 shows the TPE spectrum for the $^6P_{5/2}$ multiplet, where the symmetry assignment (lines marked with Γ_7 and Γ_8) is again that appropriate for a cubic site. The peak positions detected in the TPE spectra of Eu^{2+} are compiled in Table I for the $^6P_{7/2,5/2}$ multiplets. The luminescence data by Altshuler, Livanova, and Stolov[7] and the one-photon excitation lines by Ellens, Meijerink, and Blasse[8] are reported for comparison. All intensities are relative to the strongest line in each transition, i.e., the Γ_8 component. Because the values reported by Ref. 7 refer to emission intensities and are temperature dependent, whereas those reported by Ref. 8 reflect one-photon transition probabilities, both sets of intensity data are not directly comparable to our TPE values. Small wave number discrepancies of the peak positions can be ascribed

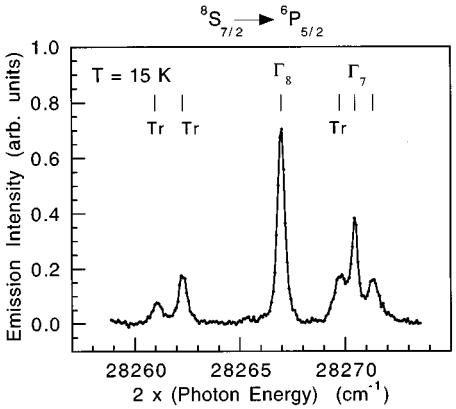

FIG. 3. Two-photon excitation spectrum of $KMgF_3$: Eu^{2+} in the $^8S_{7/2} \rightarrow {}^6P_{5/2}$ spectral range. The laser beam is linearly polarized parallel to the [010] crystal axis.

to the absolute wavelength calibration of the different experimental setup. Assignment of transitions to different irreducible representations of the cubic space group, as shown in Table I, follows that of Refs. 7 and 14, on the basis of their behavior in a magnetic field and under temperature variation.

In order to more deeply analyze the energy levels of the Eu^{2+} center in $KMgF_3$, we have reproduced in some detail the calculation scheme originally developed by O'Hare and Donlan[5] for the Gd^{3+} ion in the cubic crystal field of CaF_2, and later extended to Eu^{2+} in CaF_2 and SrF_2 crystals by Downer, Cordero-Montalvo, and Crosswhite.[11]

According to O'Hare and Donlan,[5] a good crystal-field calculation can be performed only with a set of accurate intermediate-coupling free-ion-state vectors. As a basis for a free-ion calculation, the Russell-Saunders states in the scheme $|f^7 \tau SLJM_J\rangle$, appropriate for a f^7 shell, can be used.

Starting with the wave functions of all intermediate coupled states ^8S, $^6(P,I,D)$ for the Eu^{2+} free ion, the crystal-field splitting of the states can be found. The crystal-field Hamiltonian for O_h symmetry is

$$H_{cf} = B_0^{(4)}\{C_0^{(4)} + \sqrt{\tfrac{5}{14}}(C_4^{(4)} + C_{-4}^{(4)})\} + B_0^{(6)}\{C_0^{(6)} - \sqrt{\tfrac{7}{2}}(C_4^{(6)} + C_{-4}^{(6)})\}. \quad (1)$$

Here $C_q^{(k)}$ are tensor operators proportional to spherical harmonics Y_{kq}, and $B_q^{(k)}$ are empirical coefficients determined by the charge distribution of the surrounding lattice and by the radial integrals of the f^7 electrons.

The resulting crystal-field matrix was decomposed into a 12×12 matrix for the twofold representation Γ_6, a 11×11 matrix for the twofold representation Γ_7, and a 22×22 matrix for the fourfold representation Γ_8 of cubic group. These matrices can be diagonalized and the crystal-field parameters derived from the fit of the calculated energies for the Stark components with the experimental data. This program is still in progress because, at the present time, we do not have the full set of data for the ^6I multiplet, in view of its complicated structure. Therefore we confine ourselves here only to the ^6P multiplet. Table II shows the experimental and fitted energies for both the $^6P_{7/2}$ and $^6P_{5/2}$ multiplets and the values of crystal-field parameters $B_0^{(4)}$ and $B_0^{(6)}$ used for the cubic site of Eu^{2+} in $KMgF_3$. As can be seen from Table II, the ^6P_J multiplet is well adjusted by the chosen set of crystal-field parameters, which are close to those cited in Ref. 14 The total crystal-field splitting is small in comparison with that observed for Eu^{2+} in MeF_2 (where Me stands for an alkaline-earth metal) and it is determined by the structure of the field at the site of Eu^{2+} in perovskite $KMgF_3$: its electric component is weak due to partial compensation of contributions from different coordination spheres, and the resultant effect is mainly determined by the exchange interaction.

B. Identification of trigonal europium in $KMgF_3$

The number and energy position of the measured main components of the ^6P_J multiplet indicate a crystal field of cubic symmetry and of low intensity. This is in good agreement with the hypothesis that was at the basis of the previous interpretation of Eu^{2+} ions substituting for K^+ ions in the $KMgF_3$ lattice. Substitution of the Mg^{2+} ion is ruled out by

TABLE I. Wave numbers of Stark lines of Eu^{2+} in a $KMgF_3$ crystal for the transitions $^8S_{7/2} \rightarrow {}^6P_{7/2,5/2,3/2}$. Values in cm^{-1}. Wave numbers marked with an asterisk are lines observed in emission, while the symbol Tr denotes a transition assigned to a trigonal site-symmetry.

Reference 7			Reference 8			Present work		
Peak position	Relative intensity		Relative intensity	Peak position	Relative intensity	Peak position	Relative intensity	
$T=4.2$ K			$T=77$ K	$T=4.2$ K		$T=15$ K		
				$^6P_{7/2}$ multiplet				
27 825.2	50		10	27 822.9	8	27 826.0	5	
				27 824.5				
				27 832.3	9	27 834.0	1	
27 834.5*	5		15	27 833.1	19	27 835.0	5	Tr
27 836.3*	50		20			27 836.8	13	Tr
27 839.8*	50	$^2\Gamma_6$	25	27 836.9	15	27 840.3	21	$^2\Gamma_6$
27 841.1*	0		5	27 838.5	9	27 841.5	4	Tr
						27 843.7	1	
27 845.2*	35	$^4\Gamma_8$	50	27 843.1	50	27 845.8	50	$^4\Gamma_8$
27 847.0*	15	$^2\Gamma_7$	30	27 844.7	32	27 847.3	27	$^2\Gamma_7$
27 849.5*	0		15	27 847.0	17	27 849.8	5	Tr
				$^6P_{5/2}$ multiplet				
28 251.1*			10	28 248.6				
						28 261.0	5	Tr
28 260.6*			20	28 258.2		28 262.3	14	Tr
28 265.2*	0	$^4\Gamma_8$	50	28 262.9		28 267.0	50	$^4\Gamma_8$
						28 269.7	18	Tr
28 268.7*	0	$^2\Gamma_7$	25	28 266.9		28 270.5	32	$^2\Gamma_7$
						28 271.3	14	
				$^6P_{3/2}$ multiplet				
28 670.0*								

the larger ionic radius of Eu^{2+}, with respect to that of Mg^{2+}, and by the observation that the Mg^{2+} site of octahedral symmetry should experience a much stronger crystal field. The cubo-octahedral symmetry of the K^+-ion surrounding produces a smaller crystal-field splitting, but in this case a positive-ion vacancy or other defects are necessary in order to compensate for the charge difference. The presence of a defect bound in the vicinity of the Eu^{2+} ion should lower the local symmetry, inducing a further splitting of the ^6P_J multiplet as measured in europium-doped alkali halides.[12,15,16] In $KMgF_3$, emission lines originating from Eu^{2+} ions at noncubic sites have been measured,[7,8] although at low temperature some of the lines are missing from the emission spectra and the relative intensities of the observed components are temperature dependent. In our low-temperature TPE spectra all the components of the $^6P_{7/2}$ and $^6P_{5/2}$ multiplets for different site symmetries show up fully resolved. This allowed us to carry out a number of trial calculations on the basis of an electrostatic model for a crystalline field of lower symmetry around the Eu^{2+} ion. As a result of these calculations we conclude that two kinds of site symmetry are consistent with our data: trigonal and orthorhombic. The calculated centers of gravity of the $J=\frac{7}{2}$ and $\frac{5}{2}$ manifolds are shifted to energies lower than those of the cubic centers. The set of spectral features in Table I labeled with Tr is ascribed to a trigonal site for the Eu^{2+} ion, in close analogy to the centers described by Sierro[17] and Gilfanov *et al.*[18] in MeF_2. Possessing a symmetry nearly cubic with a small axial distortion along the C_3 third-order axis, these centers reveal a relatively small crystal-field splitting, resulting in four lines for the $J=\frac{7}{2}$ manifold and three lines for the $J=\frac{5}{2}$ manifold as shown in Table I and in Figs. 2 and 3. The increase in oscillator strength for one photon f-f transitions, at sites lacking inversion symmetry, might account for the observed photoluminesence intensities, in spite of the low concentration of trigonal Eu^{2+} centers.

In addition to the electronic transitions described, one can observe also a line at 27825 ± 1 cm^{-1} that accompanies

TABLE II. Wave numbers of the $^6P_{7/2,5/2}$ Stark components and crystal-field parameters for Eu^{2+} in the $KMgF_3$ cubic site. Values in cm^{-1}.

$B_0^{(4)} = -384.2$
$B_0^{(6)} = 448.5$

$^6P_{7/2}$		$^6P_{5/2}$	
Experimental	Calculated	Experimental	Calculated
27 840.3	27 840.4	28 267.0	28 267.0
27 845.8	27 845.5	28 270.5	28 279.8
27 847.3	27 847.5		

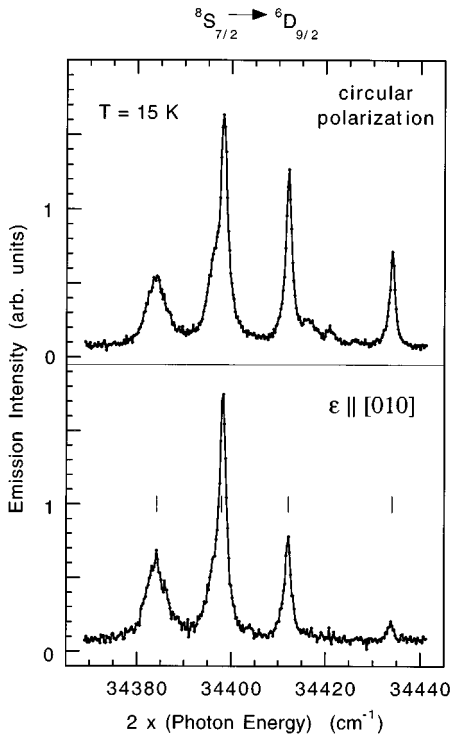

FIG. 4. Two-photon excitation spectrum of $KMgF_3$: Eu^{2+} in the spectral range of the $^8S_{7/2} \rightarrow {}^6D_{9/2}$ transitions for two different polarizations of the exciting laser beam.

each spectrum of Eu^{2+} in $KMgF_3$. This line is observed even at $T = 4$ K in luminescence,[7] and should be ascribed to a nonidentified Eu^{2+} center or a complex including the ion.

C. Detection of the states hidden by single-photon-allowed $4f^6 5d$ transitions ($^8S_{7/2} \rightarrow {}^6D_{9/2}$)

For Eu^{2+} in $KMgF_3$ the onset of the $4f^6 5d$ excitation band is immediately above the lowest ^6I_J component. The reason for such high-energy position of the center of gravity of the $4f^6 5d$ levels was discussed in Ref. 8, and connected with the ionic character of the fluorine ions and the very small crystal-field splitting for the Eu^{2+} in the K^+ site. In this case factors such as the cubic twelvefold coordination, the large distance between the rare-earth ion and the F^- ligands, the presence of a small Mg^{2+} ion in the second coordination sphere, which make the cage of the Eu^{2+} ion even larger due to a shift of F^- ligands toward the Mg^{2+} ions, provide conditions for the raising in energy of the $4f^6 5d$ levels in perovskite, as compared with the MeF_2 case. However, the higher levels of ^6I_J multiplet and the whole ^6D_J multiplet completely overlap the energy range of the intense $4f^6 5d$ one-photon-allowed absorption, and can thus be observed only by means of two-photon spectroscopy. We succeeded in this observation, and Fig. 4 shows the TPE spectra of $^8S_{7/2} \rightarrow {}^6D_{9/2}$ transitions of Eu^{2+} in $KMgF_3$ in the range of 34 360–34 440 cm^{-1}. There exist good reasons to assign a number of these lines to the Stark components of the lowest in energy of the $^8S_{7/2} \rightarrow {}^6D_J$ multiplets, namely, to the $^8S_{7/2} \rightarrow {}^6D_{9/2}$ transitions. Indeed these lines are about 6600 cm^{-1} higher than the $^6P_{7/2}$ multiplet, and about 3200 cm^{-1} higher than the ^6I_J multiplet.[8] The total crystal-field splitting for the ^6I_J multiplet, even in significantly stronger fields, as in the case of Eu^{2+} in MeF_2, is about 500 cm^{-1}, and has to be smaller in the $KMgF_3$ perovskite. Therefore the observed lines around 34 400 cm^{-1} cannot be the highest components of this multiplet. Moreover the calculated position of the lowest component of the $^6D_{9/2}$ multiplet relative to its center of gravity, as determined by the Stark splitting, is about 270 cm^{-1} in CaF_2, but the experimentally detected level is found at even higher energies.[11] Taking these considerations into account, we conclude that the observed spectrum is generated by $^8S_{7/2} \rightarrow {}^6D_{9/2}$ transitions. According to symmetry arguments this $J = \frac{9}{2}$ manifold has to be split into $^2\Gamma_6$, $^4\Gamma_8^{(1)}$, and $^4\Gamma_8^{(2)}$. The unambiguous assignment will be performed after the fit of theoretical results with experimental data which we will obtain for the ^6I_J manifold. However it is clear by now that the spectrum of $^8S_{7/2} \rightarrow {}^6D_{9/2}$ transitions also demonstrates the presence of the europium ions in different site symmetries. The data available for Eu^{2+} in $KMgF_3$ for the ^6I_J and ^6D_J multiplets are compiled in Table III.

Temperature and polarization measurements have been carried out for all spectral features under investigation. They show a strong azimuthal dependence for a linearly polarized exciting laser beam in practically all Stark components of the $^6D_{9/2}$ multiplet. The transition intensities are approximately the same when the polarization of exciting light changes from linear to circular, in contrast to the $^8S_{7/2} \rightarrow {}^6P_J$ transitions which experience an order of magnitude change. The spectral positions of the Stark components of $^6D_{9/2}$ multiplet, their full widths at half maximum, and the line shapes are strongly influenced by temperature. These effects of crystal environment are far more dramatic for $^8S_{7/2} \rightarrow {}^6D_{9/2}$ than for $^8S_{7/2} \rightarrow {}^6P_J$ transitions, and their interpretation is still object of investigation. They demonstrate only the high sensitivity of the terms to matrix truncation and the possible resonant transfer of energy between the ^6D_J and the overlapping $4f^6 5d$ electronic states. Indeed at all temperatures the measured half-width of all the lines of the $^6D_{9/2}$ multiplet is at

TABLE III. Experimental peak positions for the ^6I_J manifold and for the $^6D_{9/2}$ manifold. Values in cm^{-1}.

^6I_J manifold, $T = 4.2$ K, Ref. 8						
31 141	31 164	31 188	31 219	31 269	31 287	31 320
^6D_J manifold, $T = 15$ K, present work						
34 384	34 398	34 412	34 434			

least five times larger than that of the ^6P_J lines. These data as well as the results of measurements in the spectral range of $^8S_{7/2} \rightarrow {}^6I_J$ transitions will be discussed in more detail elsewhere.

IV. SUMMARY

Two-photon excitation spectra of Eu^{2+} in cubic perovskite $KMgF_3$ have been measured in the energy range of the $^8S_{7/2} \rightarrow {}^6P_{7/2,5/2}$ and $^8S_{7/2} \rightarrow {}^6D_{9/2}$ transitions. Compared to emission spectra or one photon excitation spectra, our TPE data on intraconfigurational transitions are of higher resolution, with linewidths smaller than 0.5 cm^{-1}, and give information on all components of each Stark multiplet. The low-temperature TPE spectra point to the existence of several sites, cubic and trigonal, for the Eu^{2+} ion, whose excess charge must be compensated for by the introduction of positive-ion vacancies.

A simplified crystal-field calculation has been performed for the cubic site with a twelvefold fluorine environment, and the results have been fitted to the experimental data of the $^6P_{7/2}$ and $^6P_{5/2}$ multiplets. In this way the $B_0^{(4)}$ and $B_0^{(6)}$ coefficients for the cubic crystal-field Hamiltonian are obtained.

The $^6D_{9/2}$ multiplet, not accessible to one-photon spectroscopy in this system, has been identified and its polarization anisotropy measured. The overlapping in energy of these levels with the broad $4f^6 5d$ states is clearly reflected by the relatively larger linewidths of the associated transitions. The unambiguous assignment of the components of the $^6D_{9/2}$ multiplet, together with a theoretical fit of the peak energies, will be possible only after detailed measurements of the ^6I_J excited states.

ACKNOWLEDGMENTS

This research was partially supported by the Istituto Nazionale di Fisica della Materia and by the Consiglio Nazionale delle Ricerche. Two of the authors (S.B. and G.G.T.) gratefully acknowledge the financial support by the University of Rome Tor Vergata, in the framework of the bilateral cooperation with the Institute of Semiconductor Physics, Kiev.

[1] M. Dagenais, M. Downer, R. Neumann, and N. Bloembergen, Phys. Rev. Lett. **46**, 561 (1981).
[2] W. A. Runciman, J. Chem. Phys. **36**, 1481 (1961).
[3] B. G. Wybourne, Phys. Rev. **148**, 317 (1966).
[4] B. R. Judd, H. M. Crosswhite, and H. Crosswhite, Phys. Rev. **169**, 130 (1968).
[5] J. M. O'Hare and V. L. Donlan, Phys. Rev. **185**, 416 (1969).
[6] S. N. Bodrug *et al.*, Opt. Spectrosc. **34**, 176 (1973).
[7] N. S. Altshuler, L. D. Livanova, and A. L. Stolov, Opt. Spectrosc. **36**, 72 (1974).
[8] A. Ellens, A. Meijerink, and G. Blasse, J. Lumin. **59**, 293 (1994).
[9] F. M. Ryan, M. Lehmann, D. W. Feldmann, and J. Murphy, J. Electrochem. Soc. **121**, 1475 (1974).
[10] M. V. Hoffman, J. Electrochem. Soc. **119**, 905 (1972).
[11] M. C. Downer, C. D. Cordero-Montalvo, and H. Crosswhite, Phys. Rev. B **28**, 4931 (1983).
[12] M. Casalboni, R. Francini, U. M. Grassano, and R. Pizzoferrato, Phys. Rev. B **34**, 2936 (1986).
[13] M. C. Downer, in *Laser Spectroscopy of Solids II*, edited by W. M. Yen, Topics in Applied Physics Vol. 65 (Springer-Verlag, Heidelberg, 1989), p. 29.
[14] N. S. Altshuler, E. Kh. Ivoilova, and A. L. Stolov, Fiz. Tverd. Tela (Leningrad) **15**, 2407 (1973) [Sov. Phys. Solid State **15**, 1602 (1974)].
[15] M. Casalboni, R. Francini, U. M. Grassano, and R. Pizzoferrato, Cryst. Latt. Def. Amorph. Mater. **16**, 261 (1987).
[16] L. A. O. Nunes, F. M. Matinaga, and J. C. Castro, Phys. Rev. B **32**, 8356 (1985).
[17] J. Sierro, J. Chem. Phys. **34**, 2183 (1961).
[18] F. Z. Gilfanov, L. D. Livanova, A. L. Stolov, and Yu. P. Khodyrev, Opt. Spectrosc. **20**, 152 (1966).